https://doi.org/10.7494/geom.2026.20.3.79

# Benefits and Limitations of InSAR-Based Monitoring of Ground Movements above Cavern Underground Gas Storage Sites: A Polish Case Study

Jan Blachowski[1], Dariusz Głąbicki[1], Piotr Grzempowski[1], Aleksandra Kaczmarek[1] *, Anna Buczyńska[1], Karolina Owczarz[1], Jörg Benndorf[2]

[1] Wrocław University of Science and Technology, Faculty of Geoengineering, Mining and Geology, Department of Geodesy and Geoinformatics, Wrocław, Poland
[2] TU Bergakademie Freiberg, Faculty of Geosciences, Geoengineering and Mining, Institute of Mine Surveying and Geodesy, Freiberg, Germany
* Corresponding author

**Abstract:** Ground displacement monitoring is a key aspect of assessing the impacts of underground gas storage (UGS). Conventional approaches are based on geodetic methods that, while providing high accuracy, are limited in spatial coverage and temporal resolution. This study assesses the suitability of synthetic aperture radar interferometry (InSAR) as a complement to standard ground displacement monitoring and identifies a method with sufficient accuracy to assess ground displacement conditions and facility safety. A comparative analysis was conducted using European Ground Motion Service (EGMS) data and independently derived Sentinel-1-based time series generated with the small baseline subset (SBAS) and persistent scatterer InSAR (PSI) methods. The analysis of a cavern UGS facility located in northern Poland spanned a five-year period from 2019 to 2023 and included error analysis and significance testing of differences between the methods. Observed displacement rates across the study area ranged from −4.3 mm/year for the SBAS method to −0.4 mm/year for PSI. Although the absolute values of the estimated velocities differed among the methods, the differences between the modeled deformation rates were statistically insignificant. The results confirm that InSAR can supplement geodetic monitoring and help investigate seasonal ground deformations associated with gas injection and withdrawal cycles as well as environmental processes, capturing patterns that discrete geodetic measurements may miss.

**Keywords:** EGMS, PSI, SBAS, comparative analysis, spatial coverage

Received: August 12, 2025; accepted: March 5, 2026



E-mails & ORCID iDs: jan.blachowski@pwr.edu.pl, https://orcid.org/0000-0003-2630-3459 (J.B.);
dariusz.glabicki@pwr.edu.pl, https://orcid.org/0000-0002-9787-4614 (D.G.);
piotr.grzempowski@pwr.edu.pl, https://orcid.org/0000-0003-0162-8759 (P.G.);
aleksandra.kaczmarek@pwr.edu.pl, https://orcid.org/0000-0003-3552-2506 (A.K.);
anna.buczynska@pwr.edu.pl, https://orcid.org/0000-0002-4440-8070 (A.B.);
karolina.owczarz@pwr.edu.pl, https://orcid.org/0000-0002-6525-1834 (K.O.);
Joerg.Benndorf@mabb.tu-freiberg.de, https://orcid.org/0000-0002-2002-8639 (J.B.).

## 1. Introduction

The importance of underground gas storage (UGS) facilities in ensuring a steady and safe energy supply is increasing, as evidenced by the growth in their volume worldwide [1, 2]. Underground storage of fluids (liquids and gases), used for industrial and heating purposes, utilizes favorable geological conditions. The most widely used underground storage types include salt caverns, depleted fields, and aquifers. The first type is developed through leaching rock salt formations to construct underground voids (caverns); the second involves storing oil and gas in depleted hydrocarbon fields; and the third involves storing gases in porous geological formations sealed from the surface with impermeable rock layers. UGS in porous rocks has the highest storage capacity of all the geological types discussed, but the pore structure prevents operation at high injection-withdrawal rates [3]. Conversely, storage in rock salt enables high operation rates. Additionally, salt caverns have a working gas capacity of 75–80% of the total storage capacity, whereas depleted field storage has a cushion gas capacity of approximately 50% of its total storage capacity. Rock salt, owing to its physical and chemical properties, serves as a natural barrier preventing leakage and contamination [4]. Details on the benefits and limitations of geological storage can be found in [2, 5–9].

Underground storage, especially caverns, causes disturbances in the rock mass that propagate to the surface. Therefore, as in underground mining, these operations require monitoring of ground displacements and the integrity of the surface technical infrastructure. The implementation of additional systems, such as those for detecting seismic activity, gas leaks, and gas dispersion, would significantly enhance UGS monitoring. Industry-standard ground monitoring methods include geodetic leveling, as well as terrestrial and satellite-based Global Navigation Satellite System (GNSS) measurements, which provide the most accurate observations but are confined to the location of control benchmarks and leveling lines. Depending on national regulations, operators are required to perform such duties either annually (Germany) or at least every five years (Poland). However, it is routine to perform ground displacement monitoring more frequently, especially during the development stage of underground storage infrastructure.

Classical geodetic leveling is recognized as the benchmark method for ground displacement monitoring and meets the requirements of national mining authorities. Methodologically, the results of leveling surveys are verifiable. Considering the level of precision obtained, implementing a semiannual to annual monitoring cycle provides a reliable approach to detecting significant ground displacements over time. The resulting ground displacement information is limited to sparsely distributed control points, usually along intersecting leveling lines. Thus, geodetic leveling being the most accurate method for monitoring vertical ground displacements, has limitations in terms of the density and spatial distribution of observation sites for precise representation of ground deformations. The accuracy of estimating ground deformations, based on leveling results, depends on the quality of the digital elevation models (DEMs) developed from them and on the differential DEM used to represent ground deformation. The quality of DEMs depends on the density and distribution of measured points, the characteristics of the topography, and the interpolation method chosen to estimate ground displacements in unmeasured locations [10]. The discrete character of information describing ground displacement based on leveling measurements may also cause irregular temporal patterns of ground movement or asymmetric deformation shapes to go undetected. Furthermore, the expansion of UGS operations over time, aimed at increasing storage capacity, requires the gradual extension of the geodetic measurement network, incorporating benchmarks that were initially placed beyond the theoretical range of influence to account for the expanding deformation zone. This poses a challenge for the spatiotemporal analysis of deformation zone evolution due to changes in the reference area regarded as stable. Finally, the seasonal operation of underground gas storage caverns may lead to oscillating vertical ground displacements associated with gas withdrawal and injection during the warm and cold seasons. These short-term movements superimpose on the long-term subsidence process related to the convergence of voids in the rock salt over time [11, 12].

The other measurement technologies that provide means to determine ground displacements include total station measurements, unmanned aerial vehicles (UAVs), light detection and ranging (LiDAR) surveys, photogrammetric surveys [13, 14], and synthetic aperture radar interferometry (InSAR). A concise comparison of their strengths and weaknesses is presented in Table 1.

The most widely used airborne methods for producing digital elevation models and monitoring ground displacement comprise aerial laser scanning (ALS) and photogrammetric surveys. The former has slightly lower accuracy but offers wider area coverage. Photogrammetric surveys are suitable for unvegetated sites, whereas LiDAR surveys penetrate vegetation cover and have a wider range of applications. A comprehensive review of UAV-based monitoring of mining areas was presented in [15–17], which discussed the benefits and limitations of active and passive UAV monitoring in these areas.

InSAR provides a complementary approach to traditional geodetic methods of ground displacement monitoring, given the growing availability of open satellite synthetic aperture radar (SAR) data, such as Sentinel-1, as well as derived displacement monitoring products like the European Ground Motion Service (EGMS). In the case of underground storage sites, InSAR can detect ground displacements over vast areas with high spatial resolution and sub-centimeter accuracy.

Since InSAR is a remote sensing method, it is necessary to compare the results with direct on-site measurements to support the verifiability of ground displacement data. To ensure validation, comparisons with geodetic leveling, fixed-point networks, or terrestrial reference targets such as corner reflectors are appropriate approaches [18]. Achievable accuracies in InSAR-based monitoring are comparable to those of geodetic leveling and fixed-point networks, allowing a monitoring cycle of half a year to one year based on cumulative analysis of shorter, 6–12-day measurement cycles.

**Table 1.** Comparison of ground displacement measurement methods

| Parameter | Method | | | | | |
|---|---|---|---|---|---|---|
| | Precise leveling | Total station (horizontal) | GNSS | UAV, LiDAR/ photogrammetry | InSAR (vertical) | InSAR (horizontal) |
| Accuracy of measurement | ±1 mm | 1.5–2 mm | ±1 mm (horizontal) ±6 mm (vertical) | 20–40 mm (horizontal) 10–20 mm (vertical) | 1–2 mm/year | 1–2 mm/year, east–west direction only |
| Accuracy of displacement determination | ±3 mm | ±5 mm | ±2 mm (horizontal) ±10 mm (vertical) | 100–120 mm (horizontal) 50–60 mm (vertical) | 3–5 mm | 3–5 mm |
| Reliability | determined by the measurement method | determined by the measurement method | determined by the measurement method | determined by the measurement method | comparison with leveling results, application of corner reflectors | comparison with horizontal geodetic network |
| Meaningful measurement interval | annual | annual | annual | 5 years or more | 0.5–1 year | 0.5–1 year |
| Data geometry/ format | point/profile | point | point coordinates | point cloud/pixel | point/pixel | point/pixel |
| Information | benchmark height difference | benchmark coordinate difference | coordinate differences ($x$, $y$, $z$) | digital elevation model | relative ground displacements, line of sight (LOS), vertical | relative ground displacements, LOS, only reliable in the east–west direction |
| Temporal frequency | low | low | low | medium | high | high |
| Benefits | highest accuracy | highest accuracy | high accuracy | medium accuracy, medium area coverage | data availability (open synthetic aperture radar (SAR) data, EGMS for the EU), high accuracy, wide area coverage, high temporal resolution | data availability (open SAR data, EGMS for the EU), wide area coverage, high temporal resolution |
| Limitations | time-consuming; limited to benchmark locations; dependent on weather | time-consuming; dependent on the weather | survey point locations only | dependent on weather; short acquisition/flight time | varied topography reduces coverage due to shadowing and layover effects; decorrelation factors; two acquisition geometries required; ambiguity in source attribution in case of multiple deformation sources | only reliable in the east–west direction; limited sensitivity; two acquisition geometries required |

In the absence of spatially congruent control points or corner reflectors, as in the case of EGMS products, spatial analysis can be applied to determine the relevant statistical metrics in the defined neighborhood around a given leveling benchmark for comparative analysis and verification [19].

A general trend toward developing frameworks for multi-tier satellite, UAV, ground, and underground monitoring systems tailored to site-specific requirements is emerging. This approach utilizes satellite data for large-scale and high-temporal-resolution remote sensing, UAV data for medium-area and high-precision monitoring, while in-situ measurements serve as validation for both data sources [17]. This results in the development of integrated ground displacement monitoring stations consisting of geodetic control for vertical and horizontal measurements, a GNSS antenna, and a corner reflector, enabling joint processing of multi-source ground movement data [20]. A laboratory setup incorporating these techniques, as well as ground settlement and tilt laser meters tested at the Institute of Mine Surveying and Geodesy (TU Bergakademie Freiberg, Germany), is shown in Figure 1.

**Fig. 1.** Integrated ground monitoring station test setup at TU Bergakademie Freiberg (phot. J. Blachowski)

Furthermore, the 6–12-day revisit time of Sentinel-1 enables monitoring of the temporal evolution of ground displacements over UGS sites, in relation to seasonal gas withdrawal and injection cycles, as well as potential environmental cycles. While numerous studies have been conducted on the applicability of InSAR to underground gas storage impact monitoring at the ground surface [21–25], each UGS site is characterized by local conditions influencing the measurements.

Thus, the aim of this study is to determine the applicability of open satellite data from the Copernicus Sentinel-1 SAR mission as a complement to standard geodetic measurements and to provide a reliable tool for monitoring ground deformation over an underground gas storage site. In this study, the ground movement data products publicly available through the EGMS within the Copernicus Land Monitoring Service (https://egms.land.copernicus.eu/), as well as ground displacements derived independently from Sentinel-1 data using the Small Baseline Subset (SBAS) InSAR time-series approach [26] and persistent scatterer InSAR (PSI) [27], have been evaluated. The assessment focused on key monitoring aspects, including spatial resolution and coverage, temporal availability, and the influence of topography on product quality, to identify ground displacements above a medium-sized cavern underground gas storage site in northern Poland.

## 2. Study Area

The area of interest (AOI) is located in northern Poland, close to the Baltic Sea and north of the cities of Gdańsk and Gdynia (Fig. 2). The mining concession covers 1.93 $km^2$, whereas the AOI, spatially congruent with the rectangular envelope of the leveling lines used for control observations of ground displacements by the cavern underground gas storage (CUGS) site operator, covers 8.69 $km^2$.

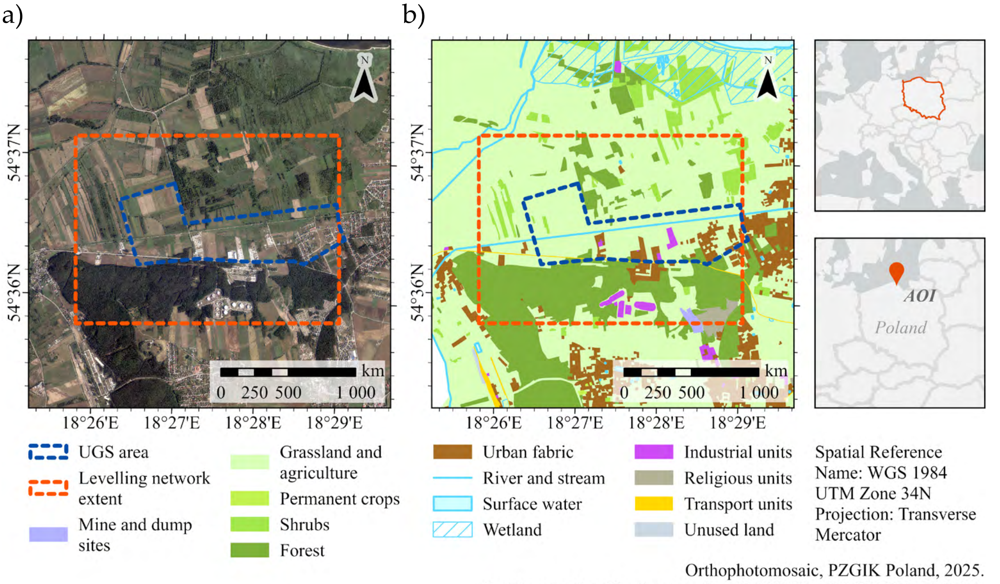


**Fig. 2.** Location of the area of interest shown with a high resolution orthophotomosaic (a) and a land cover classification (b)

The land cover to the north and west of CUGS Kosakowo consists mainly of meadows and agricultural land. Forest and industrial areas dominate in the south, whereas in the east, the main land uses are residential and service land. The distribution of the main land cover types is shown in Figure 2b. Different types of land cover create varying conditions for satellite InSAR observations, as they influence coherence values [28].

Construction of the storage facility in the Mechelinki rock salt formation began in 2009, and the first cluster of five caverns started operation five years later. Construction of the second cluster approximately 1 km east of the first was finalized in 2021. The underground caverns, leached in rock salt, are situated at a depth of approximately 970 m below ground level. The overburden is made up of Permian marine sedimentary rocks [29], Mesozoic formations (Triassic, Jurassic, and Cretaceous), and Cenozoic deposits [30].

## 3. Description of Data and Methodology

### 3.1. EGMS Products

The EGMS provides InSAR results across Europe. InSAR results are derived from Sentinel-1 SAR data by a consortium comprising four entities, using a persistent scatterer (PS) methodology, complemented by a distributed scatterer (DS) approach in areas where scatterer density does not meet quality requirements. The available EGMS ground displacement products comprise Level 2A Basic (line of sight (LOS) displacements) and Level 2B Calibrated (LOS displacements calibrated using GNSS observations) products for descending and ascending orbits, as well as the Level 3 Ortho product, obtained by decomposing the LOS displacements into vertical and horizontal (east–west) components. The Ortho products are resampled to a 100 m × 100 m grid due to coverage constraints resulting from, for example, layover effects in topographically varied areas. The data are updated annually, and at the time of the study, the product available on the EGMS Explorer [31] covered the 2019–2023 period. The EGMS update strategy follows a five-year moving-window approach. Therefore, the next available dataset will cover the 2020–2024 period. More technical details on the EGMS products can be found in [32–34]. In this study, the Level 3 (ortho) product data were used for comparative analysis with results from Sentinel-1 SAR data processed using the SBAS and PSI algorithms described in more detail in Section 3.2. The EGMS data are provided as an average of the displacements recorded at nearby PS points.

### 3.2. InSAR Processing

Interferometric processing within the scope of the study consisted of estimating ground surface displacements using two independent time-series InSAR methods, based on Sentinel-1 SAR imagery acquired over the AOI. The SAR dataset includes images from both ascending and descending acquisition orbits covering the AOI, enabling the resolution of the two-dimensional displacement field in the vertical and horizontal (east–west) directions, similar to the EGMS Ortho product. Two InSAR methods were applied for comparison: PS points were identified using the SNAP2StaMPS approach [35], while the DS analysis was performed using a modified SBAS approach [36], with interferometric noise evaluated using the MintPy software package [37]. The PSI analysis involved selecting data points exhibiting sufficiently high-amplitude dispersion in the SAR signal, focusing on point-like stable reflectors. A single-reference interferogram formation approach, applied in PSI analysis, enables the detection of PS points over man-made structures and bare rocks. The SBAS approach, on the other hand, optimizes area coverage by detecting DS points over bare soil and sparsely vegetated areas. The increased spatial coverage of the SBAS method is realized through minimizing spatial and temporal decorrelation of the phase signal, achieved by forming interferograms with short spatial and temporal baselines.

The analysis period for both the PSI and SBAS methods coincided with the EGMS data for comparative purposes. A total of 321 SAR scenes from the ascending orbit (orbit number 175), spanning the period from February 17, 2019, to August 19, 2023, as well as 208 SAR scenes from the descending orbit (orbit number 175), covering the period from February 19, 2019, to August 21, 2023, were utilized in both the PSI and SBAS processing for uniformity.

The LOS displacement time series were decomposed into vertical and horizontal (east–west) components using the approach widely described in the scientific literature [38, 39], under the assumption that the north–south component of movements can be neglected due to Sentinel-1′s near-polar orbit, which results in reduced sensitivity of the sensor in this direction. The distributed scatterer (ascending and descending) datasets derived using SBAS were resampled to a common grid for LOS projection to vertical, while the PSI datasets were combined using a vector-based approach, following the method described in [35].

### 3.3. Comparative Analysis of Ground Displacement Models

The vertical ground displacement models obtained from SBAS and PSI processing were compared with those of the EGMS Ortho model using calculated ground-movement velocities, which are independent of the displacement coordinate systems of the individual models. The points of the determined ground displacement models were resampled onto the EGMS model grid. Ground displacements at each grid node were calculated as a weighted average, where the weight was assumed to be the inverse of the distance to the grid point. The radius of the analyzed neighborhood was assumed to be 70 m. The linear trend of vertical ground displacements was calculated for each grid model node, and the least-squares method was used to approximate the trend parameters. The comparative analysis included the calculation of ground displacement velocities, along with an analysis of errors in the determined parameters, an analysis of deviations from the linear trend, and an assessment of the significance of differences between the models. The analysis was conducted to find an optimal monitoring method that minimizes displacement determination costs and provides sufficient accuracy to assess the state of ground surface deformation and the safety of the facility. Detailed time-series analyses will be the subject of a separate study.

## 4. Results

In the area covered by the leveling network, delineated by the bounding box shown in Figure 3, the EGMS model provides ground displacement values and velocities for 290 grid nodes. In the same AOI, the PSI and SBAS models provide 335 and 2036 data points, respectively. Their distribution, shown in Figure 3, is spatially congruent with the land cover types presented in Figure 2 and corresponds to areas exhibiting sufficiently high interferometric coherence.

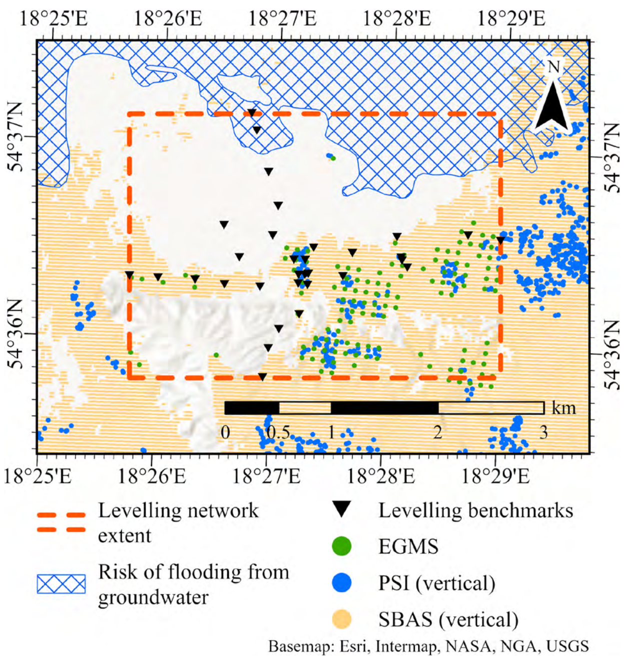


**Fig. 3.** Spatial distribution of EGMS, SBAS and PSI data points in the study area

The spatial distribution of the measurement points (MPs) is similar for the EGMS data and the SNAP2StaMPS PSI results obtained over the AOI. The SBAS results exhibit a significantly higher coverage of the AOI and a greater number of MPs than the persistent scatterer-based approaches, owing to the ability to detect distributed scatterers using small baseline interferogram processing. The PS-based approaches detect MPs only in areas with a single, stable scatterer, while the small baseline methods achieve a significantly higher MP count in non-urban areas.

Figure 4 shows a histogram of vertical ground displacement distribution in the three datasets for the 2019–2023 period. While the distributions of the EGMS and PSI products are similar, the SBAS method exhibits a significant difference in the displacement values measured over the AOI. The difference in the distribution of the histograms could be attributed to a significant number of MPs detected by SBAS in arable land and pastures, which are more sensitive to changes in soil moisture levels and subtle variations in vegetation cover. This could, in turn, cause non-zero closure-phase errors leading to phase bias in the displacement time series [40].

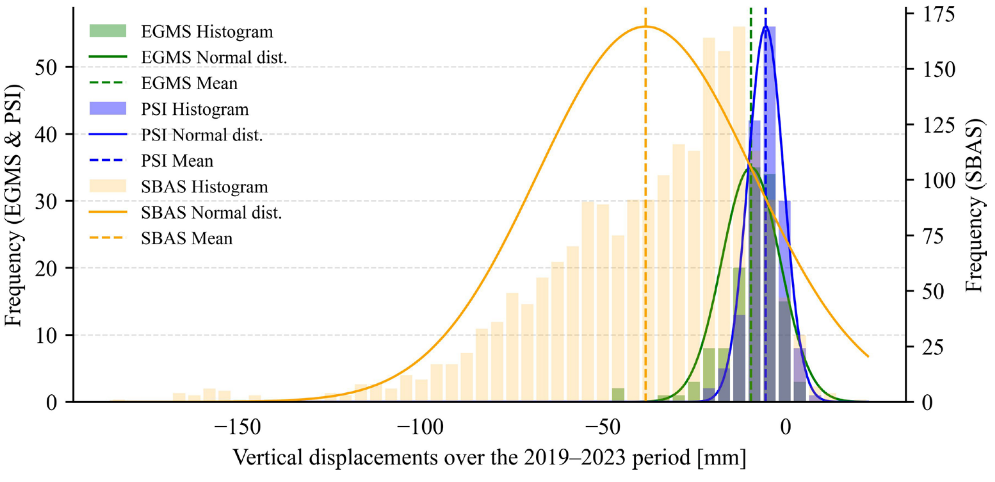


**Fig. 4.** Distribution of ground displacements from EGMS, SBAS, and PSI data

After resampling to the EGMS grid, there are 131 PSI and 288 SBAS data points available in the AOI. The lower number of points in the PSI model results from the number and spatial distribution of PS points identified for ground displacement calculations in the project. Their number and distribution are related to the location of natural persistent scatterers present predominantly in the central, eastern, and southern parts (Fig. 3). The descriptive statistics for all the considered InSAR products in the UGS area and the leveling network extent before and after resampling are shown in Table 2.

The vertical ground displacements across all examined models are negative, indicating systematic land subsidence in the AOI. The maximum registered values range from −19.7 (PSI) to −184.7 (SBAS) in the five-year period (2019–2023), with average values of −4.5 to −38.3 mm, respectively. The lowest absolute values of ground movement velocities were obtained using the PSI technique, whereas the highest were observed with the SBAS method (Table 2). Determining ground movements using the PSI technique requires careful analysis and selection of stable scatterers in each analyzed SAR image, which results in relatively lower mean errors in the time series of ground displacement estimates and lower mean errors in the approximation of movement velocities. However, meeting the stringent quality criteria for the PSI technique typically yields fewer measurement points than the SBAS technique. On the other hand, the SBAS technique provides more ground displacement measurement points over a broader spatial extent, at the cost of higher mean errors in displacement and velocity estimates.

**Table 2.** Statistical data on the available InSAR-derived ground movement products

| Parameter | EGMS product | PSI result | SBAS result |
|---|---|---|---|
| Density over the AOI (leveling extent) | 34 points/km$^2$<br>290 points total | 39 points/km$^2$<br>335 points total | 548 points/km$^2$<br>4,729 points total |
| Density over the UGS site | 28 points/km$^2$<br>54 points total | 40 points/km$^2$<br>76 points total | 393 points/km$^2$<br>757 points total |
| Number of resampled data points | as above | AOI: 16 points/km$^2$<br>UGS site: 16 points/km$^2$ | AOI: 34 points/km$^2$<br>UGS site: 32 points/km$^2$ |
| Observation period | from 2019-02-12<br>to 2023-08-20 | from 2019-02-17<br>to 2023-08-19 | from 2019-02-17<br>to 2023-08-19 |
| Observed displacement over AOI (resampled data) [mm] | max. −47.7<br>mean −9.5<br>median −7.9<br>std. dev. 7.9 | max. −19.7<br>mean −4.5<br>median −4.0<br>std. dev. 4.8 | max. −184.7<br>mean −38.3<br>median −31.7<br>std. dev. 29.6 |

Choosing the appropriate InSAR technique for ground displacement determination involves a trade-off between the required resolution and the accuracy needed to detect critical ground displacement values to monitor infrastructure safety. The differences between the results obtained with the three methods can also be attributed to the different parts of the study area covered by PSI and SBAS. Therefore, a direct comparison was performed at selected locations.

### 4.1. Comparison of Vertical Displacement Models Determined by PSI and SBAS Techniques with the EGMS Model

The calculated ground movement velocities at the EGMS grid nodes are presented in Figures 5–7 for EGMS, PSI, and SBAS results, respectively, while basic movement velocity statistics are provided in Table 3.

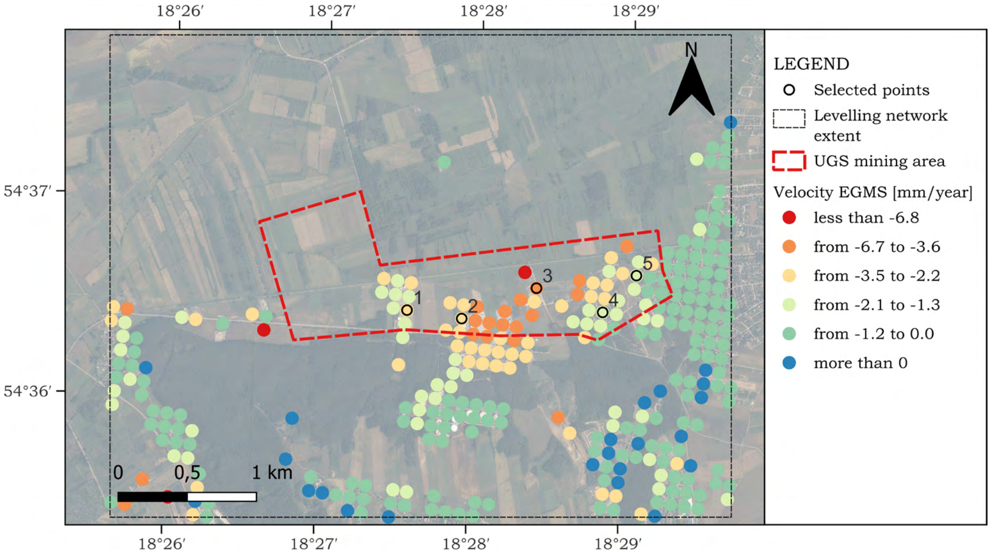


**Fig. 5.** Velocity of vertical ground movements in European Ground Motion Service grid nodes (EGMS, period 2019–2023)

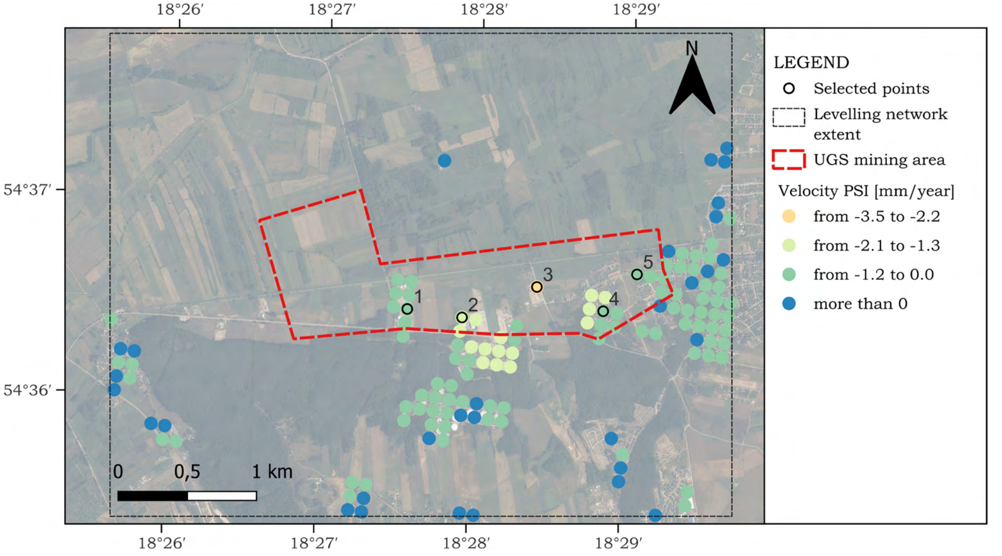


**Fig. 6.** Velocity of vertical ground movements in EGMS grid nodes determined using the PSI technique (period 2019–2023)

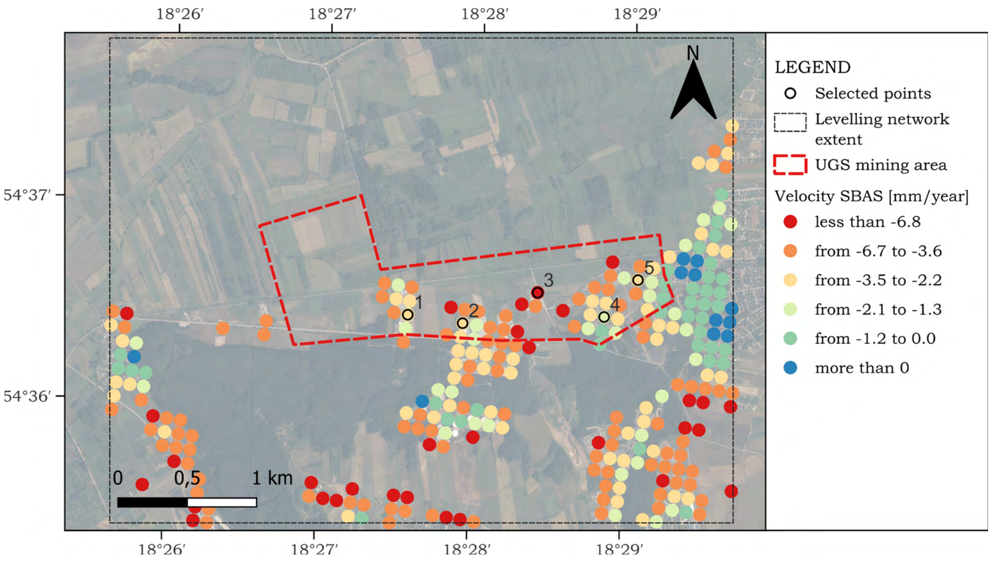


**Fig. 7.** Velocity of vertical ground movements in EGMS grid nodes determined using the SBAS technique (period 2019–2023)

**Table 3.** Basic statistics of the velocity (*V*) of ground movements for grid models

| Grid model | Min. *V* [mm/year] | Max. *V* [mm/year] | Mean *V* [mm/year] | Standard deviation of *V* [mm/year] | Number of grid points |
|---|---|---|---|---|---|
| EGMS | −9.80 | 1.9 | −1.2 | 1.41 | 290 |
| PSI | −2.70 | 0.6 | −0.4 | 0.57 | 131 |
| SBAS | −20.88 | 0.4 | −4.3 | 3.56 | 288 |

The ground movement velocities in the EGMS model in the studied area range from −9.8 mm/year to +1.9 mm/year, while in the PSI model, they range from −2.7 mm/year to +0.6 mm/year. Notably, at the extreme points of the EGMS model, PS points are missing for velocity estimation in the PSI model. In the SBAS model, the absolute values of ground movement velocities are relatively higher (from −20.8 to −0.4 mm/year) than in the other models. However, the analysis of differences, accounting for mean estimation errors and a 99% confidence interval, showed significant differences (Figs. 8, 9) at only a few points in the model.

The higher total ground displacement values and displacement velocities obtained with the SBAS technique result from using different criteria for selecting calculation points than those used in the PSI technique. These differing criteria, combined with a larger number of analyzed points, result in larger errors in the determined ground movement velocities (Tables 3, 4). At the selected points (Table 4), errors in the determined velocities of the SBAS model are within 1.2–4.4 mm/year, while in the PSI model, the corresponding errors are within 0.3–1.2 mm/year. It should be noted that vertical ground displacements in the study area during the analyzed period are relatively small compared with the estimated accuracy of determining a single displacement using the InSAR method, which is characterized by a mean error of ±5 mm (Table 2) and therefore do not indicate significant ground surface deformations.

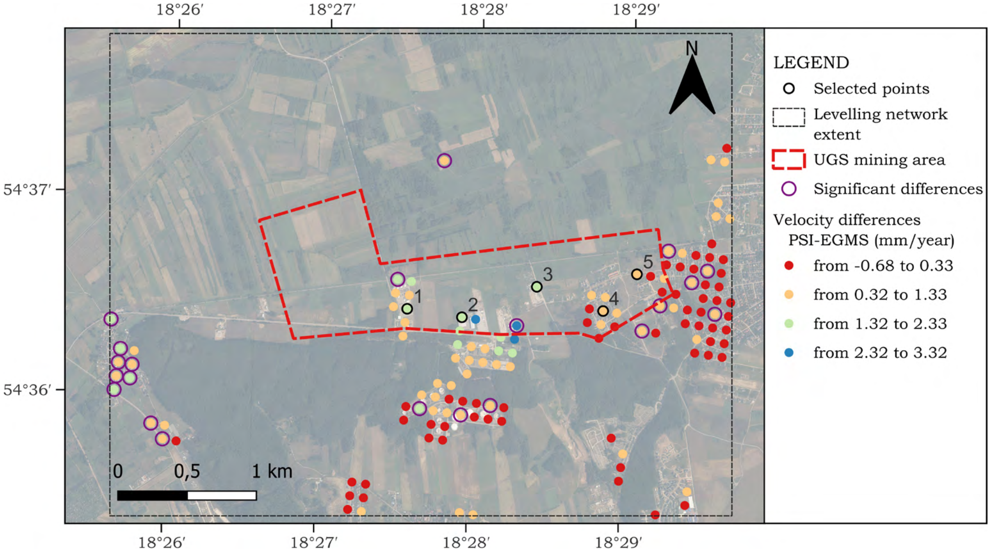


**Fig. 8.** Differences in ground movement velocity between the PSI and EGMS models

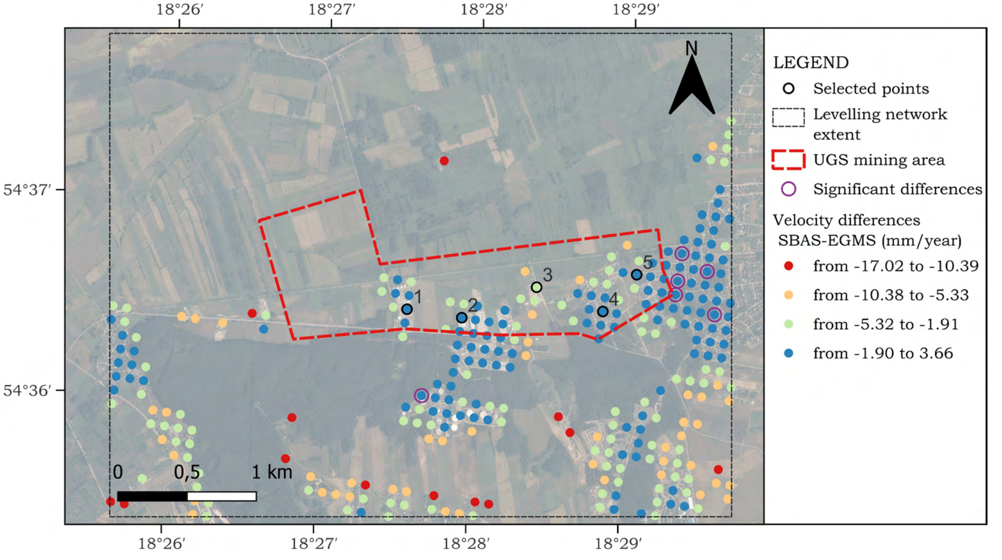


**Fig. 9.** Differences in ground movement velocity between the SBAS and EGMS models

To illustrate the results of the time series and trend comparison, five representative grid nodes were selected (Figs. 8, 9), and their list, along with the corresponding ground movement velocities and estimation errors, is presented in Table 4. Points P1 to P5 were selected in the vicinity of the leveling network benchmarks as well as significant building structures.

**Table 4.** Mean velocity (*V*) of ground movements and mean error (*m*) at selected points of grid models

| Point | $V_{EGMS}$ [mm/year] | $m_{EGMS}$ [mm/year] | $V_{PSI}$ [mm/year] | $m_{PSI}$ [mm/year] | $V_{SBAS}$ [mm/year] | $m_{SBAS}$ [mm/year] |
|---|---|---|---|---|---|---|
| P1 | −2.3 | 0.1 | −0.7 | 0.3 | −2.5 | 1.4 |
| P2 | −2.9 | 0.1 | −1.3 | 0.5 | −2.8 | 1.7 |
| P3 | −4.4 | 0.1 | −2.7 | 1.2 | −6.7 | 4.4 |
| P4 | −1.5 | 0.1 | −0.9 | 0.7 | −1.3 | 1.2 |
| P5 | −1.2 | 0.1 | −0.8 | 0.5 | −2.6 | 1.8 |

Figure 10 presents the time series of ground displacements and their trends for the representative points (P1–P5) shown in Figures 8 and 9.

The ground displacement graphs and trend lines are consistent with the directions of vertical displacements within the UGS area. Differences between ground movement velocity values are statistically insignificant. The few points with significant differences occur outside the mining area and are likely related to changes in land use (e.g., newly developed residential areas). All ground displacement velocity models indicate systematic subsidence. The velocities of vertical displacement were determined using a linear trend estimate based on the least-squares method. The mean displacement velocity errors were obtained from the variance-covariance matrix of the fitted models' parameter estimates. At selected points within the study area (Table 4), ground movement velocity values range from −1.2 to −4.4 mm/year in the EGMS model. Slightly higher values are recorded in the SBAS model, up to −6.7 mm/year, but this may be due to larger errors in determining ground displacements using this processing technique. These values are within the range of natural, large-scale vertical movements of the Earth's crust. The study area, consistent with studies of contemporary crustal movements, is undergoing steady subsidence at rates up to −3 mm/year [41]. It is not possible to clearly assess the impact of underground gas storage on the observed ground displacement, as the recorded motions and their trends have not yet exceeded the assumed confidence intervals. Additionally, an analysis of ground displacement relative to adjacent geological units is also necessary.

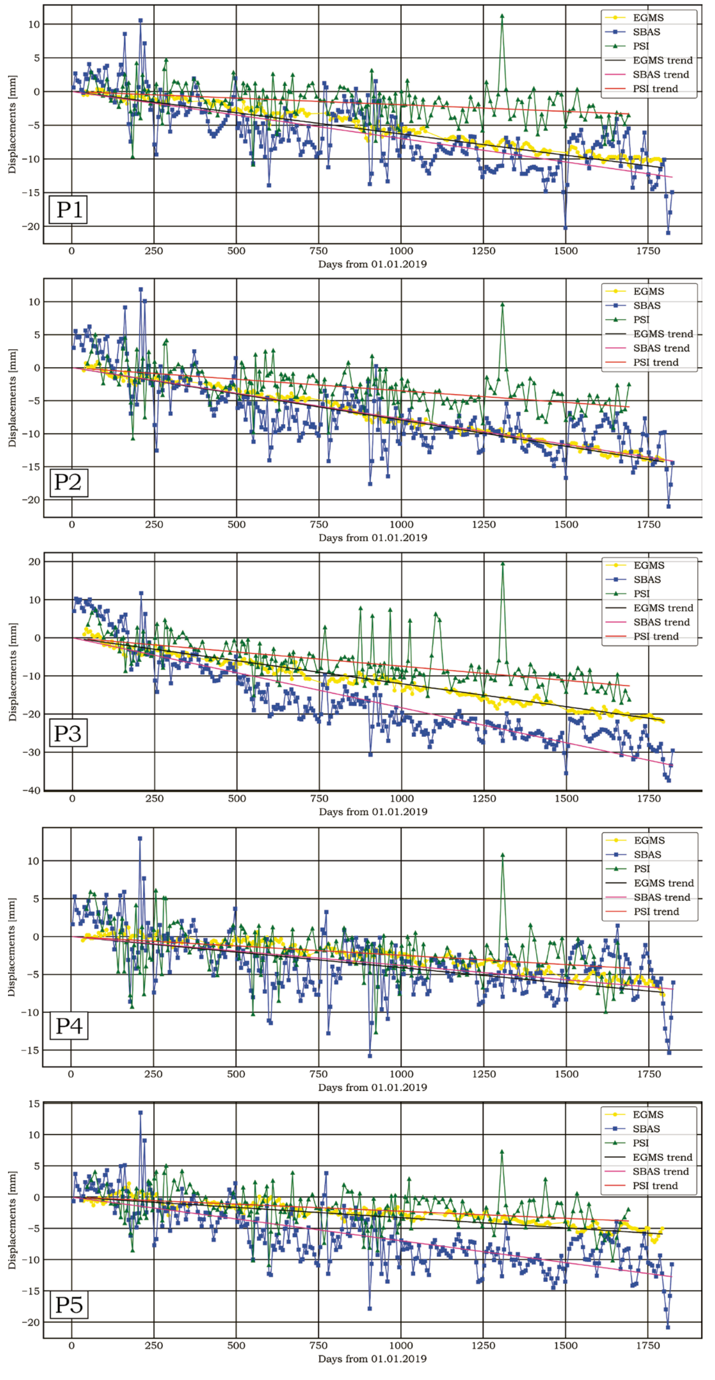


**Fig. 10.** Comparison of vertical ground displacements in EGMS grid nodes for PSI and SBAS InSAR data processing techniques with the EGMS model and their linear trends for points P1–P5

## 5. Discussion

In our study, we assessed the applicability of three different InSAR-based products for monitoring vertical ground displacements at a cavern underground gas storage site in Poland. The facility has been operating for over a decade, with rock salt leaching beginning in 2010. The temporal and spatial coverage of EGMS, PSI, and SBAS products obtained for the study area confirms their applicability as an augmentation to standard leveling-based monitoring. The number of grid data points, namely 290, 131, and 288 for EGMS, PSI, and SBAS, respectively, compared to 26 controlled leveling points in two intersecting lines (north–south and east–west), provides quasi-continuous spatial coverage of the UGS facility and adjacent areas. Nevertheless, land cover conditions (agriculture and pasture) and a small number of identified natural persistent scatterers in the AOI result in clustering of InSAR data points in certain zones, with gaps present in other parts. A proposed solution to achieve optimal performance of a monitoring system is to establish integrated monitoring stations, combining corner reflectors with leveling control points at sensitive locations, as described in the Introduction.

The literature primarily presents comparative analyses of the EGMS model with GNSS measurements at a regional scale [42, 43]. These studies indicate that displacements exceeding 1 mm/year can be detected in the EGMS model (detection threshold), and also highlight issues related to averaging values within a grid cell (e.g., spatial smoothing of local extrema). Compared to precise leveling and relative measurements, the EGMS model offers lower accuracy for individual points, but provides better spatial coverage [44]. While leveling measurements ensure higher local precision at greater cost and with limited spatial extent, the EGMS model enables the identification of deformation areas at a regional scale. Therefore, the EGMS model can complement rather than replace precise geodetic measurements [43].

EGMS, an open service providing calibrated InSAR products that requires no specialist InSAR processing knowledge or software, offers valuable details about ground surface dynamics, which can be beneficial for UGS site monitoring. However, in some use cases requiring routine monitoring with more frequent measurement intervals, it may be necessary to apply the full InSAR processing chain using a time-series approach to identify deformation patterns. This approach would be justified especially when there is a need to study a time interval exceeding the five-year period available in EGMS. Furthermore, a one-year update strategy may overlook important information on near-real-time surface changes, such as those that occur during the seasonal operation of UGS facilities.

Based on the time-series analysis of SBAS and PSI data, we determined mean ground movement velocities over the AOI to be −4.3 mm/year and −0.4 mm/year for SBAS and PSI, respectively. The maximum and mean ground movement rates obtained with the SBAS technique are higher than those from the PSI technique, possibly due to the larger number of observed scatterers and the greater dispersion of displacement values, which translates into greater deviations from the trend. Differences in ground movement velocity values between the models do not exceed the 99% confidence intervals.

Seasonal variations were observed in the time series of ground displacements determined using the SBAS method. Their presence cannot be attributed to the operation of the UGS facility. In the analyzed period, the facility did not work in cycles but maintained a consistently high inventory level. Moreover, the analysis shows that the periodic components of displacements at points within the UGS area do not differ significantly from those observed at points outside the study area. Across the entire region (including areas beyond the influence of gas storage facilities), annual fluctuating and long-term (5–10 years) components are evident. These may result from natural movements of the Earth's crust in Poland, as recorded by permanent GNSS stations.

The ground displacement values do not yet indicate the gradual manifestation of surface subsidence caused by the propagation of deformations resulting from cavern convergence, given the relatively young age of UGS operation. In salt dome workings located at shallower depths than the site under study, observed motions range from −2 to −7 mm/year [45–48].

The InSAR method is useful for assessing changes at underground gas reservoir sites relative to adjacent areas and for comparing regional-scale changes over longer periods [49]. Examining InSAR time series can also help identify and analyze seasonal trends in ground displacement rates associated with either the operational cycle of a gas storage facility or natural factors, thereby providing additional insights into the impact of CUGS on the surface. This approach was adopted in [12, 25].

A drawback of this method is the oscillation of ground displacement values relative to the trend line between successive measurements, which at the study site reach ±15 mm, and in extreme cases, 30 mm. It should be noted that deviations from the trend line are similar at selected points and occur at identical times. Because it is impossible to precisely assess the accuracy of a single measurement, it is necessary to verify vertical displacements using direct field measurements at selected points in the geodetic network. Due to a non-disclosure agreement (NDA) signed with the cavern UGS operator, the comparison of InSAR-derived ground displacements with geodetic leveling cannot be published at the present time.

## 6. Conclusions

Our study presents a comparative analysis of three InSAR-based approaches, namely EGMS, SBAS, and PSI, as a complement to geodetic leveling in the monitoring of ground displacements over an underground gas storage cavern field.

Based on the results obtained for a case study site in northern Poland, the following conclusions can be drawn.

- The mean velocities of ground movements over the AOI, determined using three different methods, range from −4.3 to −0.4 mm/year during the analyzed period, indicating systematic subsidence.
- The general trend of observed ground displacements is consistent for all three methods, although differences in magnitude were observed. In representative test locations within the study area, ground movement velocities range from −1.2 to −4.4 mm/year in the EGMS model. The values obtained with the SBAS model reach up to −6.7 mm/year. These differences are attributed to differences in processing and coherence thresholds between the methods.
- It is not yet possible to link the observed ground displacements to the impact of underground gas storage, as the observed displacements and their trends have not exceeded the assumed confidence intervals.
- PSI and SBAS methods offer higher spatial resolution and denser point distribution, providing detailed ground displacement fields suitable for localized deformation analysis. However, these approaches are sensitive to land use land cover characteristics and have limitations in vegetated areas. EGMS products offer standardized, harmonized data, currently in a five-year window, making them suitable for preliminary assessments, despite lower spatial density in rural or vegetated areas.
- Our research demonstrated that InSAR methods are an effective means of acquiring ground displacement data above underground gas storage sites, significantly increasing the temporal and spatial density of available observations.
- By comparing the values and accuracy of displacements obtained using InSAR techniques, we recommend the use of the SBAS technique when lower accuracy is acceptable but higher spatial resolution is required. The results are consistent with leveling measurements, with a mean displacement error of ±5 mm. The displacement results in the leveling network show a uniform, almost linear trend without any significant fluctuations. However, it should be noted that the measurements are taken at different intervals. While the research presented is qualitative, it allows us to identify spatial trends in displacement and potential directions for developing the leveling network and placing reference benchmarks in new locations.
- Comparison with discrete geodetic observations requires the application of spatial statistics techniques. Installation of corner reflectors and their integration with geodetic leveling networks is recommended to improve precision and data reliability.
- Last but not least, legal and internal procedures that restrict data access to the public and the scientific community, as well as the limited availability of InSAR analysis expertise on the UGS operator side, may pose constraints.

**Funding**

This research was supported by the Polish National Centre for Research and Development (grant number WPN/4/67/CLEAR/2022) and by the Federal Ministry of Education and Research of Germany (grant number 01DS22004A) as part of the bilateral project Closed-Loop Impact Monitoring for Environmentally and Socially Acceptable Energy Transition in Rural Regions (acronym: CLEAR).

**CRediT Author Contribution**

J. Blachowski: conceptualization, funding acquisition, project administration, writing – review & editing, supervision.

D. G.: data curation, formal analysis, investigation, resources.

P. G.: formal analysis, investigation, visualization, validation.

A. K.: visualization, writing – original draft, writing – review & editing.

A. B.: supervision, writing – review & editing.

K. O.: formal analysis, investigation, resources.

J. Benndorf: conceptualization, funding acquisition, methodology.

**Declaration of Competing Interests**

The authors declare that they have no known competing financial interests or personal relationships that could have appeared to influence the work reported in this paper.

**Data Availability**

Public data: The Sentinel-1 collection downloaded from the Alaska Satellite Facility (https://asf.alaska.edu) and the EGMS data downloaded from the EGMS Explorer (https://egms.land.copernicus.eu).

Restricted data: The calculated SBAS and PSI ground movement products.

Requests for access to the data sets generated or analyzed in this research will be considered upon inquiries to the corresponding author.

**Use of Generative AI and AI-Assisted Technologies**

No generative AI or AI-assisted technologies were employed in the preparation of this manuscript.

**Acknowledgments**

We acknowledge the support of the CUGS Kosakowo industrial partner in the research.

## References

[1] Ikäheimo J., Lindroos T.J., Kiviluoma J.: *Impact of climate and geological storage potential on feasibility of hydrogen fuels*. Applied Energy, vol. 342, 2023, 121093. https://doi.org/10.1016/j.apenergy.2023.121093.

[2] Tackie-Otoo B.N., Haq M.B.: *A comprehensive review on geo-storage of $H_2$ in salt caverns: Prospect and research advances*. Fuel, vol. 356, 2024, 129609. https://doi.org/10.1016/j.fuel.2023.129609.

[3] Fibbi G., Landini N., Intrieri E., Del Ventisette C., Del Soldato M.: *Open-source InSAR data to detect ground displacement induced by underground gas storage reservoirs*. Earth Systems and Environment, vol. 9(4), 2025, pp. 3083–3100. https://doi.org/10.1007/s41748-025-00593-3.

[4] Kaczmarek A., Blachowski J.: *Remote sensing perspective on monitoring and predicting underground energy sources storage environmental impacts: Literature review*. Remote Sensing, vol. 17(15), 2025, 2628. https://doi.org/10.3390/rs17152628.

[5] Xiao T., Chen T., Ma Z., Tian H., Meguerdijian S., Chen B., Pawar R., Huang L., Xu T., Cather M., McPherson B.: *A review of risk and uncertainty assessment for geologic carbon storage*. Renewable and Sustainable Energy Reviews, vol. 189, 2024, 113945. https://doi.org/10.1016/j.rser.2023.113945.

[6] Liu H., Yang C., Liu J., Hou Z., Xie Y., Shi X.: *An overview of underground energy storage in porous media and development in China*. Gas Science and Engineering, vol. 117, 2023, 205079. https://doi.org/10.1016/j.jgsce.2023.205079.

[7] National Research Council: *Induced Seismicity Potential in Energy Technologies*. The National Academies Press, Washington 2013. https://doi.org/10.17226/13355.

[8] Metz B., Davidson O., de Coninck H., Loos M., Meyer L. (eds.): *IPCC Special Report on Carbon Dioxide Capture and Storage* [prepared by Working Group III of the Intergovernmental Panel on Climate Change]. Cambridge University Press, Cambridge 2005.

[9] Evans D.J.: *An appraisal of underground gas storage technologies and incidents, for the development of risk assessment methodology*. British Geological Survey Open Report, OR/07/023, Keyworth, Nottingham 2007.

[10] Gong J., Li Z., Zhu Q., Sui H., Zhou Y.: *Effects of various factors on the accuracy of DEMs: An intensive experimental investigation*. Photogrammetric Engineering & Remote Sensing, vol. 66(8), 2000, pp. 1113–1117.

[11] Li M., Zhang H., Xing W., Hou Z., Were P.: *Study of the relationship between surface subsidence and internal pressure in salt caverns*. Environmental Earth Sciences, vol. 73(11), 2015, pp. 6899–6910. https://doi.org/10.1007/s12665-015-4405-8.

[12] Fibbi G., Montalti R., Del Soldato M., Cespa S., Ferretti A., Fanti R.: *Unlocking the InSAR potential for managing underground gas storage in salt caverns*. International Journal of Applied Earth Observation and Geoinformation, vol. 141, 2025, 104656. https://doi.org/10.1016/j.jag.2025.104656.

[13] Zhang T., Zhang W., Yang R., Cao D., Chen L., Li D., Meng L.: *$CO_2$ injection deformation monitoring based on UAV and InSAR technology: A case study of Shizhuang town, Shanxi province, China*. Remote Sensing, vol. 14(1), 2022, 237. https://doi.org/10.3390/rs14010237.

[14] Ćwiąkała P., Gruszczyński W., Stoch T., Puniach E., Mrocheń D., Matwij W., Matwij K., Nędzka M., Sopata P., Wójcik A.: *UAV applications for determination of land deformations caused by underground mining*. Remote Sensing, vol. 12(11), 2020, 1733. https://doi.org/10.3390/rs12111733.

[15] Ren H., Zhao Y., Xiao W., Hu Z.: *A review of UAV monitoring in mining areas: Current status and future perspectives*. International Journal of Coal Science & Technology, vol. 6(3), 2019, pp. 320–333. https://doi.org/10.1007/s40789-019-00264-5.

[16] Pawlik M., Haske B., Flores H., Bernsdorf B., Rudolph T.: *Towards a long-term unmanned aerial vehicle (UAV) monitoring framework for post-mining effects: Prosper-Haniel case*. Mining, vol. 4(2), 2024, 211–229. https://doi.org/10.3390/mining4020013.

[17] Haske B., Rudolph T., Bernsdorf B., Pawlik M.: *Innovative environmental monitoring methods using multispectral UAV and satellite data*. First Break, vol. 42(2), 2024, pp. 41–47. https://doi.org/10.3997/1365-2397.fb2024012.

[18] Cigna F., Esquivel Ramírez R., Tapete D.: *Accuracy of Sentinel-1 PSI and SBAS InSAR displacement velocities against GNSS and geodetic leveling monitoring data*. Remote Sensing, vol. 13(23), 2021, 4800. https://doi.org/10.3390/rs13234800.

[19] Głąbicki D.: *Displacement forecasting in mining areas using satellite SAR interferometry and machine learning*. Wrocław University of Science and Technology, Wrocław 2023 [PhD thesis].

[20] Spreckels V., Engel T.: *Set-up and application of multisensor-referencestations (MSST) for levelling, GNSS and InSAR in the former mining regions Saarland and Ruhrgebiet within Germany*, [in:] *5th Joint International Symposium on Deformation Monitoring: JISDM 2022: Proceedings: 20–22 June 2022, Polytechnic City of Innovation, Valencia (Spain)*, Editorial Universitat Politècnica de València, Valencia 2023, pp. 645–658.

[21] Ferretti A., Tamburini A., Novali F., Fumagalli A., Falorni G., Rucci A.: *Impact of high resolution radar imagery on reservoir monitoring*. Energy Procedia, vol. 4, 2011, pp. 3465–3471. https://doi.org/10.1016/j.egypro.2011.02.272.

[22] Struhár J., Rapant P., Kačmařík M., Hlaváčová I., Lazecký M.: *Monitoring non-linear ground motion above underground gas storage using GNSS and PSInSAR based on Sentinel-1 data*. Remote Sensing, vol. 14(19), 2022, 4898. https://doi.org/10.3390/rs14194898.

[23] Fibbi G., Beni T., Fanti R., Del Soldato M.: *Underground gas storage monitoring using free and open source InSAR data: A case study from Yela (Spain)*. Energies, vol. 16(17), 2023, 6392. https://doi.org/10.3390/en16176392.

[24] Priolo E., Zinno I., Guidarelli M., Romanelli M., Lanari R., Sandron D., Garbin M., Peruzza L., Romano M. A., Zuliani D., Tunini L., Magrin A.: *The birth of an underground gas storage in a depleted gas reservoir – results from integrated seismic and ground deformation monitoring*. Earth and Space Science, vol. 11(11), 2024, e2023EA003275. https://doi.org/10.1029/2023EA003275.

[25] Fibbi G., Novellino A., Bateson L., Fanti R., Del Soldato M.: *Multidisciplinary assessment of seasonal ground displacements at the Hatfield Moors gas storage site in a peat bog landscape*. Scientific Reports, vol. 14(1), 2024, 22521. https://doi.org/10.1038/s41598-024-73548-9.

[26] Li S., Xu E., Li Z.: *Review of the SBAS InSAR time-series algorithms, applications, and challenges*. Geodesy and Geodynamics, vol. 13(2), 2022, pp. 114–126. https://doi.org/10.1016/j.geog.2021.09.007.

[27] Ferretti A., Prati C., Rocca F.: *Permanent scatterers in SAR interferometry*. IEEE Transactions on Geoscience and Remote Sensing, vol. 39(1), 2001, pp. 8–20. https://doi.org/10.1109/36.898661.

[28] Maghsoudi Y., Hooper A. J., Wright T. J., Lazecky M., Ansari H.: *Characterizing and correcting phase biases in short-term, multilooked interferograms*. Remote Sensing of Environment, vol. 275, 2022, 113022. https://doi.org/10.1016/j.rse.2022.113022.

[29] Marcinkowska A., Ochtyra A., Olędzki J.R., Wołk-Musiał E., Zagajewski B.: *Mapa geomorfologiczna województw pomorskiego i warmińsko-mazurskiego z wykorzystaniem metod geoinformatycznych*. Teledetekcja Środowiska, t. 49, 2013, pp. 43–79.

[30] Cała M., Cyran K., Kowalski M., Wilkosz P.: *Influence of the anhydrite interbeds on a stability of the storage caverns in the Mechelinki salt deposit (northern Poland)*. Archives of Mining Sciences, vol. 63(4), 2018, pp. 1007–1025. https://doi.org/10.24425/ams.2018.124990.

[31] European Ground Motion Service (EGMS): *Ortho – vertical component 2016-present (vector), Europe, yearly, Aug. 2022*. EEA Geospatial Data Catalogue, 2022. https://doi.org/10.2909/4a14a29b-7db7-40e4-81ad-df3aa8dfbc6f [access: March 30, 2026].

[32] Costantini M., Minati F., Trillo F., Ferretti A., Novali F., Passera E., Dehls J., Larsen Y., Marinkovic P., Eineder M., Brcic R., Siegmund R., Kotzerke P., Probeck M., Kenyeres A., Proietti S., Solari L., Andersen H.S.: *European Ground Motion Service (EGMS)*, [in:] *IGARSS 2021 – 2021 IEEE International Geoscience and Remote Sensing Symposium: Proceedings: 12–16 July, 2021, Virtual Symposium, Brussels, Belgium*, IEEE, 2021, pp. 3293–3296. https://doi.org/10.1109/IGARSS47720.2021.9553562.

[33] Copernicus Land Monitoring Service: *European Ground Motion Service*. https://land.copernicus.eu/en/products/european-ground-motion-service?tab=overview [access: July 15, 2025].

[34] Copernicus Land Monitoring Service: *European Ground Motion Service (EU-GMS) – A proposed Copernicus service element: White paper*. September 21, 2017. https://land.copernicus.eu/en/products/european-ground-motion-service/egms-white-paper/@@download/file [access: July 15, 2025].

[35] Foumelis M., Blasco J. M. D., Desnos Y.-L., Engdahl M., Fernandez D., Veci L., Lu J., Wong C.: *ESA SNAP – stamps integrated processing for Sentinel-1 persistent scatterer interferometry*, [in:] *IGARSS 2018 – 2018 IEEE International Geoscience and Remote Sensing Symposium: Proceedings: July 22–27, 2018, Valencia, Spain*, IEEE, 2018, pp. 1364–1367. https://doi.org/10.1109/IGARSS.2018.8519545.

[36] Berardino P., Fornaro G., Lanari R., Sansosti E.: *A new algorithm for surface deformation monitoring based on small baseline differential SAR interferograms*. IEEE Transactions on Geoscience and Remote Sensing, vol. 40(11), 2003, pp. 2375–2383. https://doi.org/10.1109/TGRS.2002.803792.

[37] Yunjun Z., Fattahi H., Amelung F.: *Small baseline InSAR time series analysis: Unwrapping error correction and noise reduction*. Computers & Geosciences, vol. 133, 2019, 104331. https://doi.org/10.1016/j.cageo.2019.104331.

[38] Wright T.J., Parsons B.E., Lu Z.: *Toward mapping surface deformation in three dimensions using InSAR*. Geophysical Research Letters, vol. 31(1), 2004, L01607. https://doi.org/10.1029/2003GL018827.

[39] Fuhrmann T., Garthwaite M.C.: *Resolving three-dimensional surface motion with InSAR: Constraints from multi-geometry data fusion*. Remote Sensing, vol. 11(3), 2019, 241. https://doi.org/10.3390/rs11030241.

[40] Karami E., Shami S., Maghsoudi Y., Ranjgar B., Azadnejad S.: *Investigating the InSAR phase bias in the SBAS algorithm and its effect on different landcovers*. IEEE Access, vol. 13, 2025, pp. 82514–82526. https://doi.org/10.1109/ACCESS.2025.3568144.

[41] Kowalczyk K.: *Cały kraj się obsuwa*. Geodeta, vol. 8(135), 2006, pp. 45–48.

[42] Cardello G.L., Barreca G., Monaco C., de Michele M., Antonioli R.: *First comparison of subsidence/uplift rates between Copernicus European Ground Motion Service data and long-term MIS 5.5 geological record in Mediterranean regions*. Earth-Science Reviews, vol. 265, 2025, 105132. https://doi.org/10.1016/j.earscirev.2025.105132.

[43] Even M., Westerhaus M., Kutterer H.: *German and European Ground Motion Service: A comparison*. PFG – Journal of Photogrammetry, Remote Sensing and Geoinformation Science, vol. 92(3), 2024, pp. 253–270. https://doi.org/10.1007/s41064-024-00273-3.

[44] Vradi A., Sala J., Solari L., Balasis-Levinsen J.: *Validating the European Ground Motion Service: An assessment of measurement point density*. The International Archives of the Photogrammetry, Remote Sensing and Spatial Information Sciences, vol. XLVIII-4-W7-2023, 2023, pp. 247–252. https://doi.org/10.5194/isprs-archives-XLVIII-4-W7-2023-247-2023.

[45] Chrzanowski A., Szostak-Chrzanowski A., Bastin G., Lutes J.: *Monitoring and modelling of ground subsidence in mining areas – case studies*. Geomatica, vol. 54(4), 2000, pp. 405–413. https://doi.org/10.5623/geomat-2000-0056.

[46] Kortas G., Maj A.: *Deformations of the protection shelf in the "Wapno" Salt Mine, based on model studies*. Archives of Mining Sciences, vol. 59(4), 2014, pp. 869–886. https://doi.org/10.2478/amsc-2014-0060.

[47] Hejmanowski R., Malinowska A.: *Land subsidence inversion method application for salt mining-induced rock mass movement*. Gospodarka Surowcami Mineralnymi – Mineral Resources Management, vol. 33(3), 2017, pp. 179–200. https://doi.org/10.1515/gospo-2017-0034.

[48] Maj A.: *Pomiar ruchu górotworu w kopalniach soli*. Prace Instytutu Mechaniki Górotworu PAN, vol. 24(1–4), 2022, pp. 61–70.

[49] Kim T.T.H., Tran H.H., Bui K.L., Lipecki T.: *Mining-induced land subsidence detected by Sentinel-1 SAR images: An example from the historical Tadeusz Kościuszko salt mine at Wapno, Greater Poland Voivodeship, Poland*. Inżynieria Mineralna – Journal of the Polish Mineral Engineering Society, vol. 1(2), 2021. https://doi.org/10.29227/IM-2021-02-04.